Journal of Computational and Applied Mathematics 365 (2020) 112374

Contents lists available at ScienceDirect

Journal of Computational and Applied Mathematics

journal homepage: www.elsevier.com/locate/cam

On accuracy of approximate boundary and distributed H^1 shape gradient flows for eigenvalue optimization ☆

Shengfeng Zhu [a,*], Xianliang Hu [b], Qingbiao Wu [b]

[a] School of Mathematical Sciences, East China Normal University, Shanghai 200241, China
[b] School of Mathematical Sciences, Zhejiang University, HangZhou 310027, China

ARTICLE INFO

Article history:
Received 23 January 2019
Received in revised form 16 June 2019

Keywords:
Shape optimization
Eigenvalue
Shape gradient flow
Distributed shape gradient
Finite element
Error estimate

ABSTRACT

The boundary and distributed shape gradients of elliptic eigenvalues in shape optimization are approximated by the finite element method. We show a priori error estimates for the two approximate shape gradients in H^1 shape gradient flows. The convergence analysis shows that the volume integral formula converges faster and offers higher accuracy when the finite element method is used for discretization. Numerical results verify the theory for the Dirichlet case. Shape optimization examples solved by algorithms illustrate the more effectiveness of distributed shape gradients for the Dirichlet case. For optimizing a Neumann eigenvalue, the boundary and volume H^1 flows have the same efficiency. Moreover, we observe that the distributed H^1 shape gradient flow is more efficient than the boundary L^2 shape gradient flow in literature.

1. Introduction

Eigenvalue problems in optimal shape design have fundamental importance for science and engineering, especially in structural mechanics (see. e.g., [1–8]). A *structure theorem* was built by Zolésio for general shape functionals on general domains. By the structure theorem, the Eulerian derivative can be expressed as a concise boundary integral. The boundary formulation of Eulerian derivative has been used widely in numerical algorithms [4,7]. But it actually fails to hold when the boundary is not smooth enough. The Eulerian derivative can be expressed as a domain integral, which is more general than the boundary formulation [4]. These two formulations of Eulerian derivatives are equivalent through integration by parts if the boundary is regular enough.

The effectiveness and high accuracy of the boundary Eulerian derivative for solving shape optimization problems has been shown, when the solver is based on the spectral methods of particular solution [9–12] (see [13,14] for highly accurate numerical methods of particular solution for computing the eigenpairs on polygonal domains in 2D). Thus, in that case, the boundary Eulerian derivative is very effective and allows the dimension reduction of calculating the shape gradient just by evaluating surface integrals, instead of volume integrals of the distributed shape gradient.

Comparing with the (meshless) methods of particular solution, the finite element method is a mesh-type method. It is widely used to discretize the PDE constraints for shape gradient computations in shape optimization (see e.g. [15,16]). This approach based on domain triangulation is flexible to shape representation and shape changes. The sensitivity

☆ This work was supported in part by the National Natural Science Foundation of China (Grant Nos. 11201153, 11571115, 11632015, and 11771393), Natural Science Foundation of Shanghai (Grant No. 19ZR1414100), Science and Technology Commission of Shanghai Municipality (No. 18dz2271000), and Natural Science Foundation of Zhejiang Province (Grant No. LZ14A010002).

* Corresponding author.
E-mail addresses: sfzhu@math.ecnu.edu.cn (S. Zhu), xlhu@zju.edu.cn (X. Hu), qbwu@zju.edu.cn (Q. Wu).

https://doi.org/10.1016/j.cam.2019.112374
0377-0427/

information-directional derivatives of objective functions and constraints needs to be very accurately computed in order for the optimization algorithms to fully converge [17]. For finite element approximations of eigenvalue optimization, the boundary shape gradients are widely used (see e.g., [1,2,4–7,18]). The boundary expression of Eulerian derivative, although popular, is actually not suitable for use since the finite element solution does not have the appropriate smoothness under which the boundary integral formula can be obtained (pp. 531 [4]). The use of domain expressions is natural and promising. Recently, Hiptmair et al. [19] showed that the finite element approximations of distributed shape gradients converge faster and are more accurate than the boundary versions for linear elliptic problems. Similar behaviors are shown for shape optimization in the Stokes equation [20]. But convergence of shape gradients is not performed in "real" descent direction in optimization algorithms. We refer to [21–23] for more applications of the distributed shape gradients. To best of our knowledge, no literature reported numerical shape optimization examples with comparisons shows that the distributed shape gradients are more effective. For shape optimization of Dirichlet eigenvalue problems [24], our numerical evidence shows that the algorithm using the distributed shape gradients is more initially independent. *A priori* error estimates are obtained in an infinite-dimensional operator norm [25]. The volume formulation of Eulerian derivative offers more accuracy [25]. To ensure the "real" descent direction in optimization algorithms, convergence analysis should be performed for discretizations of the popular H^1 shape gradient flows, which are used in algorithms of [24]. H^1 shape gradient flows have been actually used widely in shape design and topology optimization (see e.g., [16,22–24]).

In this paper, we prove convergence for Galerkin finite element approximations of H^1 shape gradient flows in eigenvalue optimization. Both boundary and distributed shape gradients are considered with comparisons. Numerical results are presented for verifying convergence of approximate shape gradients as well as effectiveness of shape gradient algorithms. The rest of the paper is organized as follows. The Laplace eigenvalue optimization problems are presented in Section 2. Finite element approximations of H^1 shape gradient flows associated with boundary and volume Eulerian derivatives are given. In Section 3, we present a priori error estimates in H^1 and L^2 norms for H^1 shape gradient flows. In Section 4, numerical results are presented. Brief conclusions are drawn in Section 5.

2. Finite element approximations of H^1 shape gradient flows for eigenvalue optimization

In shape gradient algorithms for shape optimization, it is desirable to introduce auxiliary flows for increasing the smoothness of descent/ascent directions. The H^1 shape gradient flow is typically useful for regularization [22,24]. We first introduce the eigenvalue problem and the Eulerian derivatives in shape optimization. Then, we present finite element approximations of H^1 shape gradient flows for eigenvalue optimization.

2.1. H^1 shape gradient flows in eigenvalue optimization

Let Ω be a bounded domain in $\mathbb{R}^d$ ($d = 2, 3$) with Lipschitz continuous boundary $\partial\Omega$. We consider the Laplace eigenvalue problem:

$$\begin{cases} -\Delta u = \lambda u & \text{in } \Omega \\ u = 0 \quad \text{or} \quad \dfrac{\partial u}{\partial n} = 0 & \text{on } \partial\Omega. \end{cases} \tag{1}$$

We consider the eigenvalue problems in shape optimization [2,3,5,6,18]:

$$\min_{|\Omega|=\mathcal{C}} \lambda \ \text{(Dirichlet)} \quad \text{and} \quad \max_{|\Omega|=\mathcal{C}} \lambda \ \text{(Neumann)}, \tag{2}$$

where $|\Omega|$ denotes the geometric measure of Ω and $\mathcal{C} > 0$ is a prescribed number.

We recall basic shape calculus using the speed method (Section 2.9, pp. 54 and pp. 98 of [7]) for solving (2). For a variable $t \in [0, \tau)$ with $\tau > 0$, we introduce a velocity field $\mathcal{V}(t, x) \in C([0, \tau]; \mathcal{D}^1(\mathbb{R}^d, \mathbb{R}^d))$ with $\mathcal{D}^1(\mathbb{R}^d, \mathbb{R}^d)$ being the space of continuously differentiable transformations of $\mathbb{R}^d$. Then, we define a family of transformations $T_t : \Omega \to \Omega_t$ with $\Omega_t = T_t(\mathcal{V})(\Omega)$. For $x = x(t, X) \in \Omega_t$ with $X \in \Omega$, it satisfies

$$\frac{\mathrm{d}x}{\mathrm{d}t}(t, X) = \mathcal{V}(t, x(t, X)), \quad x(0, X) = X. \tag{3}$$

Denote $\mathcal{V}_n = \mathcal{V}(0)|_{\partial\Omega} \cdot n$.

The variational formulation of (1) is to find $\lambda \in \mathbb{R}$, $0 \neq u \in V$ such that

$$(\nabla u, \nabla v) = \lambda(u, v) \quad \forall v \in V, \tag{4}$$

where $V = H_0^1(\Omega)$ ($V = H^1(\Omega)$) for the Dirichlet (Neumann) boundary condition. It is well-known that there exists a sequence of eigenpairs of (4). For a simple eigenvalue λ, let (λ, u) be an eigenpair of (4). Then, $\lambda(\Omega)$ is shape differentiable and we have the Eulerian derivative (see e.g., [24,25] for derivations)

$$\lambda'(\Omega; \mathcal{V})_\Omega = \int_\Omega \left[-2\nabla u \cdot \mathrm{D}\mathcal{V}\nabla u + \mathrm{div}\mathcal{V}(|\nabla u|^2 - \lambda u^2)\right]\mathrm{d}x, \tag{5}$$

where $D\mathcal{V}$ denotes the Jacobian of $\mathcal{V}$. If, furthermore, Ω is convex or if it is of class C^2, then the boundary Eulerian derivative of Dirichlet eigenvalue

$$\lambda'(\Omega;\mathcal{V})_{\partial\Omega} = -\int_{\partial\Omega}\left(\frac{\partial u}{\partial n}\right)^2 \mathcal{V}_n \mathrm{d}s. \tag{6}$$

Let ∇_Γ denote *tangential gradient*. If Ω is of class C^3 for the Neumann case, then

$$\lambda'(\Omega;\mathcal{V})_{\partial\Omega} = \int_{\partial\Omega}\left(|\nabla_\Gamma u|^2 - \lambda u^2\right)\mathcal{V}_n \mathrm{d}s, \tag{7}$$

The H^1 shape gradient flows we consider are the two variational formulations associated with two different Eulerian derivatives:

$$\text{find } \mathcal{U}^V \in H^1(\Omega)^d \text{ such that } A(\mathcal{U}^V,\mathcal{V}) = -\lambda'(\Omega;\mathcal{V})_\Omega \quad \forall\, \mathcal{V}\in H^1(\Omega)^d \tag{8}$$

and

$$\text{find } \mathcal{U}^B \in H^1(\Omega)^d \text{ such that } A(\mathcal{U}^B,\mathcal{V}) = -\lambda'(\Omega;\mathcal{V})_{\partial\Omega} \quad \forall\, \mathcal{V}\in H^1(\Omega)^d, \tag{9}$$

where the bilinear form $A(\cdot,\cdot): H^1(\Omega)^d \times H^1(\Omega)^d \to \mathbb{R}$ is defined as

$$A(\mathcal{U},\mathcal{V}) := \int_\Omega (D\mathcal{U} : D\mathcal{V} + \mathcal{U}\cdot\mathcal{V})\mathrm{d}x \quad \forall\, \mathcal{U},\mathcal{V}\in H^1(\Omega)^d$$

with $D\mathcal{U} : D\mathcal{V} = \sum_{i,j=1}^d \partial_j\mathcal{U}_i\partial_j\mathcal{V}_i$.

2.2. Finite element approximations of H^1 shape gradient flows

We consider the standard Ritz–Galerkin finite element method [26,27] for discretization of the variational formulations (4), (8) and (9). For the shape gradient deformation algorithm we shall present, the domain Ω here at each iteration is naturally assumed to be a polygon/polyhedron, which can be triangulated exactly with no geometric error introduced. Consider a family of triangulations $\{\mathcal{T}_h\}_{h>0}$ satisfying that $\overline{\Omega} = \cup_{K\in\mathcal{T}_h}\overline{K}$, where the mesh size $h := \max_{K\in\mathcal{T}_h} h_K$ with $h_K := \mathrm{diam}\{K\}$ for any $K\in\mathcal{T}_h$. Let $\{V_h\}_{h>0}$ be a family of finite-dimensional subspaces of $H_0^1(\Omega)$. For the linear Lagrange elements, $V_h := \{v_h \in C^0(\overline{\Omega})\cap H_0^1(\Omega) : v_h|_K \in \mathbb{P}_1(K)\ \forall K\in\mathcal{T}_h\}$ in the Dirichlet case with $\mathbb{P}_1(K)$ denoting the set of piecewise linear polynomials on K and $V_h = \{v_h \in C^0(\overline{\Omega}) : v_h|_K \in \mathbb{P}_1(K)\ \forall K\in\mathcal{T}_h\}$ in the Neumann case. Throughout, we shall denote by C a general constant, which may differ at different occurrences and depend on the eigenvalue and the mesh aspect ratio, but is always independent of h. We assume that the mesh family $\{\mathcal{T}_h\}_{h>0}$ is *regular* so that the following approximation property holds [26]:

$$\inf_{v_h\in V_h}(\|u-v_h\|_{L^2(\Omega)} + h\|\nabla u - \nabla v_h\|_{L^2(\Omega)}) \le Ch^2|u|_{H^2(\Omega)} \quad \forall u\in H^2(\Omega). \tag{10}$$

Suppose moreover that the mesh is *quasi-uniform*, i.e., $\min_{K\in\mathcal{T}_h} h_K \ge Ch\ \forall h>0$, based on which the *inverse inequality* holds (see e.g. Theorem 4.5.11 [26]).

The weak formulation for conforming finite element approximation of the problem (4) reads: find $\lambda_h\in\mathbb{R}$ and $0\neq u_h\in V_h$ such that

$$(\nabla u_h,\nabla v_h) = \lambda_h(u_h,v_h) \quad \forall v_h\in V_h, \tag{11}$$

For (11), there exist a finite sequence of eigenvalues

$$0<\lambda_{1,h}\le\lambda_{2,h}\le\cdots\le\lambda_{N,h}, \quad N=\dim\ V_h,$$

and corresponding eigenvectors

$$u_{1,h}, u_{2,h}\ldots u_{N,h},$$

which can be assumed to satisfy

$$(u_{i,h},u_{j,h}) = \delta_{ij}. \tag{12}$$

In the following, we omit the index number of a specific eigenvalue/eigenfunction for simplicity. Let (λ_h,u_h) be an eigenpair of (11). We refer to [25] for convergence analysis of shape gradients associated with the multiple eigenvalue case. We have the following *a priori* error estimates on approximating eigenvalues and eigenfunctions ([28] and Theorem 5.1 [29]).

Lemma 1. *Assume that Ω is a convex polygon/polyhedron or C^2 domain and $\{\mathcal{T}_h\}_{h>0}$ are quasi-uniform. Then,*

$$\lambda\le\lambda_h\le\lambda + Ch^2|u|_{H^2(\Omega)},$$

and

$$\|u-u_h\|_{L^2(\Omega)}+h\|\nabla u-\nabla u_h\|_{L^2(\Omega)}\le Ch^2|u|_{H^2(\Omega)}.$$

Let $\boldsymbol{V}_h=\{\boldsymbol{v}_h\in[C^0(\bar{\Omega})]^d|\boldsymbol{v}_h|_K\in\mathbb{P}_1(K)^d\ \forall K\in\mathcal{T}_h\}\subset H^1(\Omega)^d$. The finite-dimensional approximations of (8) and (9) read respectively as

$$\text{find}\ \ \mathcal{U}_h^V\in\boldsymbol{V}_h\ \ \text{such that}\ A(\mathcal{U}_h^V,\mathcal{V}_h)=-\lambda'(\Omega;\mathcal{V}_h)_{\Omega,h}\quad\forall\,\mathcal{V}_h\in\boldsymbol{V}_h \tag{13}$$

and

$$\text{find}\ \ \mathcal{U}_h^B\in\boldsymbol{V}_h\ \ \text{such that}\ A(\mathcal{U}_h^B,\mathcal{V}_h)=-\lambda'(\Omega;\mathcal{V}_h)_{\partial\Omega,h}\quad\forall\,\mathcal{V}_h\in\boldsymbol{V}_h, \tag{14}$$

where

$$\lambda'(\Omega;\mathcal{V}_h)_{\Omega,h}:=\int_\Omega\left[-2\nabla u_h\cdot\mathrm{D}\mathcal{V}_h\nabla u_h+\mathrm{div}\mathcal{V}_h(|\nabla u_h|^2-\lambda_h u_h^2)\right]\mathrm{d}x$$

and

$$\lambda'(\Omega;\mathcal{V}_h)_{\partial\Omega,h}:=-\int_{\partial\Omega}\left(\frac{\partial u_h}{\partial n}\right)^2\mathcal{V}_h\cdot n\mathrm{d}s\quad\left(\text{or}\ \int_{\partial\Omega}\left(|\nabla_\Gamma u_h|^2-\lambda_h u_h^2\right)\mathcal{V}_h\cdot n\mathrm{d}s\right)$$

denote the finite element approximations of $\lambda'(\Omega;\mathcal{V})_\Omega$ and $\lambda'(\Omega;\mathcal{V})_{\partial\Omega}$, respectively.

3. Convergence analysis

In this part, We perform convergence analysis with a priori error estimates for finite element approximations of H^1 shape gradient flows associated with both boundary and volume expressions of Eulerian derivatives. We consider the Dirichlet case for simplicity. It may be generalized similarly to the Neumann case.

Let us first define the Ritz projection $P_h: H_0^1(\Omega)\to V_h$ such that

$$(\nabla P_h u,\nabla v_h)=(\nabla u,\nabla v_h)\quad\forall v_h\in V_h. \tag{15}$$

Lemma 2. *Let assumptions in Lemma 1 hold. Then,*

$$\|\nabla(P_h u-u_h)\|_{L^2(\Omega)}\le Ch^2|u|_{H^2(\Omega)}.$$

Proof. We take $v_h=P_hu-u_h$ in (4), (11) and (15). Then, we have

$$\begin{aligned}(\nabla(P_hu-u_h),\nabla(P_hu-u_h))&=(\lambda u-\lambda_h u_h,P_hu-u_h)\\&=\big(\lambda(u-u_h)+(\lambda-\lambda_h)u_h,P_hu-u_h\big).\end{aligned}$$

Then, by the Cauchy–Schwarz inequality and triangle inequality,

$$\begin{aligned}\|\nabla(P_hu-u_h)\|_{L^2(\Omega)}^2&\le\big(\lambda\|u-u_h\|_{L^2(\Omega)}+|\lambda-\lambda_h|\|u_h\|_{L^2(\Omega)}\big)\|P_hu-u_h\|_{L^2(\Omega)}\\&=\big(\lambda\|u-u_h\|_{L^2(\Omega)}+|\lambda-\lambda_h|\big)\|P_hu-u_h\|_{L^2(\Omega)}\\&\le C\big(\lambda\|u-u_h\|_{L^2(\Omega)}+|\lambda-\lambda_h|\big)\|\nabla(P_hu-u_h)\|_{L^2(\Omega)},\end{aligned}$$

where the normalization fact that $\|u_h\|_{L^2(\Omega)}=1$ and the Poincaré inequality are used in the last inequality. Therefore,

$$\begin{aligned}\|\nabla(P_hu-u_h)\|_{L^2(\Omega)}&\le C\big(\lambda\|u-u_h\|_{L^2(\Omega)}+|\lambda-\lambda_h|\big)\\&\le C\big(\lambda Ch^2+Ch^2\big)|u|_{H^2(\Omega)}\\&\le Ch^2|u|_{H^2(\Omega)}\end{aligned} \tag{16}$$

using Lemma 1. □

Lemma 3. *Assume that $u\in W^{2,4}(\Omega)$. Then,*

$$\|\nabla u-\nabla u_h\|_{L^4(\Omega)}\le Ch|u|_{W^{2,4}(\Omega)}. \tag{17}$$

Proof. By triangle inequality, we have

$$\|\nabla u-\nabla u_h\|_{L^4(\Omega)}\le\|\nabla u-\nabla P_hu\|_{L^4(\Omega)}+\|\nabla P_hu-\nabla u_h\|_{L^4(\Omega)}. \tag{18}$$

By (8.5.4) on pp. 230 [26] and the approximation property (4.4.28) on pp. 110 [26],

$$\begin{aligned}\|\nabla u-\nabla P_hu\|_{L^4(\Omega)}&\le C\inf_{v\in V_h}\|\nabla u-\nabla v\|_{L^4(\Omega)}\\&\le Ch|u|_{W^{2,4}(\Omega)},\end{aligned} \tag{19}$$

By inverse inequality and Lemma 2, we have

$$\begin{aligned}\|\nabla P_h u - \nabla u_h\|_{L^4(\Omega)} &\le Ch^{-\frac{d}{4}}\|\nabla P_h u - \nabla u_h\|_{L^2(\Omega)}\\ &\le Ch^{2-\frac{d}{4}}|u|_{H^2(\Omega)}.\end{aligned} \tag{20}$$

A combination of (18), (19) and (20) allows the conclusion to hold. □

Lemma 4. *Let Ω be a C^2 domain. Let (λ, u) be a simple eigenpair of (4). Assume that $u \in W^{2,4}(\Omega)$. Then, there exists a unique solution $\mathcal{U}^V \in H^1(\Omega)^d$ of (8) such that*

$$\|\mathcal{U}^V\|_{H^2(\Omega)} \le C\kappa|u|^2_{W^{2,4}(\Omega)},$$

where κ denotes the mean curvature on $\partial\Omega$.

Proof. The bilinear form $A(\cdot,\cdot)$ is obviously continuous and coercive on $H^1(\Omega)^d$. By Lax–Milgram theorem, there exists a unique solution $\mathcal{U}^V \in H^1(\Omega)^d$ for (8). Moreover, we get

$$\begin{aligned}\|\mathcal{U}^V\|^2_{H^1(\Omega)} &\le A(\mathcal{U}^V, \mathcal{U}^V)\\ &= \int_\Omega \left[2\nabla u \mathrm{D}\mathcal{U}^V \nabla u - \operatorname{div}\mathcal{U}^V(|\nabla u|^2 - \lambda u^2)\right]\mathrm{d}x\\ &\le 2\|\nabla u\|_{L^2(\Omega)}\|\mathrm{D}\mathcal{U}^V\|_{L^2(\Omega)}\|\nabla u\|_{L^\infty(\Omega)} + \|\operatorname{div}\mathcal{U}^V\|_{L^2(\Omega)}\||\nabla u|^2 - \lambda u^2\|_{L^2(\Omega)},\end{aligned}$$

which implies the *a priori* estimate

$$\|\mathcal{U}^V\|_{H^1(\Omega)} \le C\left(\|\nabla u\|_{L^2(\Omega)}\|\nabla u\|_{L^\infty(\Omega)} + \|\nabla u\|^2_{L^4(\Omega)} + \lambda\|u\|^2_{L^4(\Omega)}\right).$$

Furthermore, we have from (8) using the fact that $u \in H^2(\Omega)$, Green's theorem, and $\frac{\partial u}{\partial x_i} = \frac{\partial u}{\partial n}n_i$ on $\partial\Omega$

$$\begin{cases} -\Delta\mathcal{U}_i + \mathcal{U}_i = -2\operatorname{div}\left(\dfrac{\partial u}{\partial x_i}\nabla u\right) + \dfrac{\partial}{\partial x_i}(|\nabla u|^2 - \lambda u^2) = 0 \quad \text{in } \Omega\\ \dfrac{\partial\mathcal{U}_i}{\partial n} = 2\dfrac{\partial u}{\partial x_i}\dfrac{\partial u}{\partial n} - |\nabla u|^2 n_i = |\nabla u|^2 n_i \quad \text{on } \partial\Omega,\end{cases} \tag{21}$$

where $\mathcal{U}^V = (\mathcal{U}_i)_{i=1}^d$ and $n = (n_i)_{i=1}^d$ for $i = 1, 2, \ldots, d$. Then, the standard regularity estimate (see e.g., [26]) for elliptic problems implies that

$$\|\mathcal{U}_i\|_{H^2(\Omega)} \le C\||\nabla u|^2 n_i\|_{H^{\frac{1}{2}}(\partial\Omega)}.$$

Let b be the oriented distance function associated with Ω satisfying $\nabla b|_{\partial\Omega} = n$ and $\kappa = \operatorname{div} n$ (see Chapter 6 [4]). We have $b \in H^2(\Omega)$ since Ω is C^2. By the trace theorem, triangle inequality and Cauchy–Schwarz inequality, we have

$$\begin{aligned}\|\mathcal{U}_i\|_{H^2(\Omega)} &\le C\left\||\nabla u|^2\frac{\partial b}{\partial x_i}\right\|_{H^1(\Omega)}\\ &\le C\left(\left\||\nabla u|^2\frac{\partial b}{\partial x_i}\right\|_{L^2(\Omega)} + \left\|2\nabla^2 u\nabla u\frac{\partial b}{\partial x_i}\right\|_{L^2(\Omega)} + \left\||\nabla u|^2\nabla\frac{\partial b}{\partial x_i}\right\|_{L^2(\Omega)}\right)\\ &\le C|u|^2_{W^{1,\infty}(\Omega)}|b|_{H^1(\Omega)} + C|u|_{W^{2,4}(\Omega)}|u|_{W^{1,\infty}(\Omega)}|\nabla b|_{L^4(\Omega)} + C|u|^2_{W^{1,\infty}(\Omega)}|b|_{H^2(\Omega)}\\ &\le C|u|^2_{W^{2,4}(\Omega)}|b|_{H^2(\Omega)},\end{aligned}$$

where Sobolev embedding theorems are used. □

Theorem 1. *Let assumptions in Lemma 4 hold. Then,*

$$\|\mathcal{U}^V - \mathcal{U}_h^V\|_{L^2(\Omega)} + h\|\mathcal{U}^V - \mathcal{U}_h^V\|_{H^1(\Omega)} \le Ch^2|u|^2_{W^{2,4}(\Omega)}.$$

Proof. We first prove the error estimate in the H^1 norm. Let us define a family of Lagrange interpolation operators $\mathcal{I}_h : \boldsymbol{V} \cap C^0(\bar{\Omega})^d \to \boldsymbol{V}_h$, which satisfy

$$\|\mathcal{U} - \mathcal{I}_h\mathcal{U}\|_{H^1(\Omega)} \le Ch|\mathcal{U}|_{H^2(\Omega)} \quad \forall\, \mathcal{U} \in H^2(\Omega). \tag{22}$$

Since by the triangle inequality, (22), and Lemma 4

$$\|\mathcal{U}^V - \mathcal{U}_h^V\|_{H^1(\Omega)} \le \|\mathcal{U}^V - \mathcal{I}_h\mathcal{U}^V\|_{H^1(\Omega)} + \|\mathcal{I}_h\mathcal{U}^V - \mathcal{U}_h^V\|_{H^1(\Omega)} \tag{23}$$

what left is to estimate $\|\mathcal{I}_h\mathcal{U}^V - \mathcal{U}_h^V\|_{H^1(\Omega)}$. Denote $\mathcal{X}_h := \mathcal{I}_h\mathcal{U}^V - \mathcal{U}_h^V$. We first have

$$\begin{aligned}\|\mathcal{X}_h\|_{H^1(\Omega)}^2 &= A(\mathcal{X}_h, \mathcal{X}_h)\\ &= A(\mathcal{I}_h\mathcal{U}^V - \mathcal{U}^V, \mathcal{X}_h) + A(\mathcal{U}^V - \mathcal{U}_h^V, \mathcal{X}_h)\\ &= A(\mathcal{I}_h\mathcal{U}^V - \mathcal{U}^V, \mathcal{X}_h) - \lambda'(\Omega; \mathcal{X}_h)_\Omega + \lambda'(\Omega; \mathcal{X}_h)_{\Omega,h}.\end{aligned} \tag{24}$$

By continuity and (22), (24) implies that

$$\begin{aligned}\|\mathcal{X}_h\|_{H^1(\Omega)}^2 &\le \|\mathcal{I}_h\mathcal{U}^V - \mathcal{U}^V\|_{H^1(\Omega)}\|\mathcal{X}_h\|_{H^1(\Omega)} + |\lambda'(\Omega; \mathcal{X}_h)_\Omega - \lambda'(\Omega; \mathcal{X}_h)_{\Omega,h}|\\ &\le Ch|\mathcal{U}^V|_{H^2(\Omega)}\|\mathcal{X}_h\|_{H^1(\Omega)} + |\lambda'(\Omega; \mathcal{X}_h)_\Omega - \lambda'(\Omega; \mathcal{X}_h)_{\Omega,h}|,\end{aligned} \tag{25}$$

in which

$$\begin{aligned}|\lambda'(\Omega; \mathcal{X}_h)_\Omega - \lambda'(\Omega; \mathcal{X}_h)_{\Omega,h}| \le &\left|\int_\Omega 2(\nabla u \cdot \mathrm{D}\mathcal{X}_h\nabla u - \nabla u_h \cdot \mathrm{D}\mathcal{X}_h\nabla u_h)\mathrm{d}x\right|\\ + &\left|\int_\Omega \operatorname{div}\mathcal{X}_h((|\nabla u|^2 - \lambda u^2) - (|\nabla u_h|^2 - \lambda_h u_h^2))\mathrm{d}x\right|.\end{aligned} \tag{26}$$

We estimate the two terms on the R.H.S. of (26). For the first term, we have

$$\begin{aligned}&\left|\int_\Omega 2(\nabla u \cdot \mathrm{D}\mathcal{X}_h\nabla u - \nabla u_h \cdot \mathrm{D}\mathcal{X}_h\nabla u_h)\mathrm{d}x\right|\\ =&\left|\int_\Omega\Big[2\nabla u \cdot \mathrm{D}\mathcal{X}_h(\nabla u - \nabla u_h) + 2(\nabla u - \nabla u_h)\cdot \mathrm{D}\mathcal{X}_h\nabla u - 2(\nabla u - \nabla u_h)\cdot \mathrm{D}\mathcal{X}_h(\nabla u - \nabla u_h)\Big]\mathrm{d}x\right|\\ =&\left|\int_\Omega 2(\nabla u - \nabla u_h)\cdot(\mathrm{D}\mathcal{X}_h + \mathrm{D}\mathcal{X}_h^T)\nabla u\mathrm{d}x - \int_\Omega(\nabla u - \nabla u_h)\cdot(\mathrm{D}\mathcal{X}_h + \mathrm{D}\mathcal{X}_h^T)(\nabla u - \nabla u_h)\mathrm{d}x\right|\\ \le&2\left|\int_\Omega(\nabla u - \nabla u_h)\cdot(\mathrm{D}\mathcal{X}_h + \mathrm{D}\mathcal{X}_h^T)\nabla u\mathrm{d}x\right| + \left|\int_\Omega(\nabla u - \nabla u_h)\cdot(\mathrm{D}\mathcal{X}_h + \mathrm{D}\mathcal{X}_h^T)(\nabla u - \nabla u_h)\mathrm{d}x\right|\\ \le&C\|\nabla u - \nabla u_h\|_{L^4(\Omega)}\|\mathrm{D}\mathcal{X}_h\|_{L^2(\Omega)}(\|\nabla u\|_{L^4(\Omega)} + \|\nabla u - \nabla u_h\|_{L^4(\Omega)})\\ \le&Ch|u|_{W^{2,4}(\Omega)}\|\mathcal{X}_h\|_{H^1(\Omega)}(|u|_{W^{1,4}(\Omega)} + Ch|u|_{W^{2,4}(\Omega)}),\end{aligned} \tag{27}$$

where Lemma 3 was used in last inequality. For the second term, we have

$$\begin{aligned}&\left|\int_\Omega \operatorname{div}\mathcal{X}_h((|\nabla u|^2 - \lambda u^2) - (|\nabla u_h|^2 - \lambda_h u_h^2))\mathrm{d}x\right|\\ \le&\|\operatorname{div}\mathcal{X}_h\|_{L^2(\Omega)}\big(\||\nabla u|^2 - |\nabla u_h|^2\|_{L^2(\Omega)} + \|\lambda u^2 - \lambda_h u_h^2\|_{L^2(\Omega)}\big)\\ \le&C\|\mathcal{X}_h\|_{H^1(\Omega)}\Big(2\|\nabla u\|_{L^4(\Omega)}\|\nabla u - \nabla u_h\|_{L^4(\Omega)} + \|\nabla u - \nabla u_h\|_{L^4(\Omega)}^2\\ &+ |\lambda - \lambda_h|\|u\|_{L^4(\Omega)}^2 + \lambda_h\|u - u_h\|_{L^4(\Omega)}(\|u - u_h\|_{L^4(\Omega)} + 2\|u\|_{L^4(\Omega)})\Big)\\ \le&C\|\mathcal{X}_h\|_{H^1(\Omega)}\Big(2\|\nabla u\|_{L^4(\Omega)}\|\nabla u - \nabla u_h\|_{L^4(\Omega)} + \|\nabla u - \nabla u_h\|_{L^4(\Omega)}^2\\ &+ |\lambda - \lambda_h|\|u\|_{L^4(\Omega)}^2 + \lambda_h\|u - u_h\|_{H^1(\Omega)}(\|u - u_h\|_{H^1(\Omega)} + 2\|u\|_{L^4(\Omega)})\Big)\end{aligned} \tag{28}$$

using the Cauchy–Schwarz inequality, triangle inequality and Sobolev embedding theorem. By *a priori* error estimates in Lemmas 1 and 3, (28) implies that

$$\left|\int_\Omega \operatorname{div}\mathcal{X}_h((|\nabla u|^2 - \lambda u^2) - (|\nabla u_h|^2 - \lambda_h u_h^2))\mathrm{d}x\right| \le C\|\mathcal{X}_h\|_{H^1(\Omega)}h|u|_{W^{2,4}(\Omega)}^2. \tag{29}$$

A combination of (26), (27), and (29) implies that

$$|\lambda'(\Omega; \mathcal{X}_h)_\Omega - \lambda'(\Omega; \mathcal{X}_h)_{\Omega,h}| \le C\|\mathcal{X}_h\|_{H^1(\Omega)}h|u|_{W^{2,4}(\Omega)}^2. \tag{30}$$

Thus, we obtain from (25), (30) and Lemma 4

$$\|\mathcal{X}_h\|_{H^1(\Omega)} \le Ch|u|_{W^{2,4}(\Omega)}^2. \tag{31}$$

Now we prove L^2 error estimate $\|\mathcal{U}^V - \mathcal{U}_h^V\|_{L^2(\Omega)}$. Let $\widetilde{\mathcal{U}}$ be the solution of the continuous problem with perturbated R.H.S. corresponding to its discrete formulation (13):

$$\text{find } \widetilde{\mathcal{U}} \in H^1(\Omega)^d \quad \text{such that } A(\widetilde{\mathcal{U}}, \mathcal{V}) = -\lambda'(\Omega; \mathcal{V})_{\Omega,h} \quad \forall\, \mathcal{V} \in H^1(\Omega)^d, \tag{32}$$

which is well-posed by Lax–Milgram theorem. Then, the Galerkin orthogonality reads:

$$A(\widetilde{\mathcal{U}} - \mathcal{U}_h^V, \mathcal{V}_h) = 0 \quad \forall \mathcal{V}_h \in \boldsymbol{V}_h.$$

By the triangle inequality,

$$\|\mathcal{U}^V - \mathcal{U}_h^V\|_{L^2(\Omega)} \le \|\mathcal{U}^V - \widetilde{\mathcal{U}}\|_{L^2(\Omega)} + \|\widetilde{\mathcal{U}} - \mathcal{U}_h^V\|_{L^2(\Omega)}. \tag{33}$$

In order to bound $\|\mathcal{U}^V - \widetilde{\mathcal{U}}\|_{L^2(\Omega)}$, we introduce an auxiliary problem with the Laplacian operating componentwise:

$$\begin{cases} -\Delta\Phi + \Phi = \mathcal{U}^V - \widetilde{\mathcal{U}} & \text{in } \Omega \\ \dfrac{\partial \Phi}{\partial n} = 0 & \text{on } \partial\Omega, \end{cases} \tag{34}$$

which is well-posed and has the *a priori* estimate

$$\|\Phi\|_{H^2(\Omega)} \le C\|\mathcal{U}^V - \widetilde{\mathcal{U}}\|_{L^2(\Omega)}. \tag{35}$$

We have

$$\begin{aligned} \|\mathcal{U}^V - \widetilde{\mathcal{U}}\|^2_{L^2(\Omega)} &= A(\mathcal{U}^V - \widetilde{\mathcal{U}}, \Phi) \\ &= |\lambda'(\Omega; \Phi)_{\Omega,h} - \lambda'(\Omega; \Phi)| \\ &\le Ch^2|u|_{W^{2,4}(\Omega)}|\Phi|_{H^2(\Omega)}, \end{aligned} \tag{36}$$

where the last inequality can be obtained similarly by modifying proof arguments (26)–(30) with $\mathcal{X}_h \in H^1(\Omega)^d$ replaced by $\Phi \in H^2(\Omega)^d$ (we omit details for simplicity). From (35) and (36), thus

$$\|\mathcal{U}^V - \widetilde{\mathcal{U}}\|_{L^2(\Omega)} \le Ch^2|u|_{W^{2,4}(\Omega)}.$$

To estimate $\|\widetilde{\mathcal{U}} - \mathcal{U}_h^V\|_{L^2(\Omega)}$, we first introduce a dual problem

$$\text{find } \ \mathcal{Z} \in H^1(\Omega)^d \ \text{ such that } A(\mathcal{V}, \mathcal{Z}) = (\widetilde{\mathcal{U}} - \mathcal{U}_h^V, \mathcal{V}) \quad \forall \mathcal{V} \in H^1(\Omega)^d,$$

which has the *a priori* estimate

$$\|\mathcal{Z}\|_{H^2(\Omega)} \le C\|\widetilde{\mathcal{U}} - \mathcal{U}_h^V\|_{L^2(\Omega)}. \tag{37}$$

Then

$$\begin{aligned} \|\widetilde{\mathcal{U}} - \mathcal{U}_h^V\|^2_{L^2(\Omega)} &= A(\widetilde{\mathcal{U}} - \mathcal{U}_h^V, \mathcal{Z}) \\ &= A(\widetilde{\mathcal{U}} - \mathcal{U}_h^V, \mathcal{Z} - \mathcal{I}_h\mathcal{Z}) \\ &\le C\|\widetilde{\mathcal{U}} - \mathcal{U}_h^V\|_{H^1(\Omega)}\|\mathcal{Z} - \mathcal{I}_h\mathcal{Z}\|_{H^1(\Omega)} \\ &\le Ch\|\widetilde{\mathcal{U}} - \mathcal{U}_h^V\|_{H^1(\Omega)}|\mathcal{Z}|_{H^2(\Omega)} \qquad \text{(by (22))}. \end{aligned} \tag{38}$$

By (37) and (38), we get

$$\begin{aligned} \|\widetilde{\mathcal{U}} - \mathcal{U}_h^V\|_{L^2(\Omega)} &\le Ch\|\widetilde{\mathcal{U}} - \mathcal{U}_h^V\|_{H^1(\Omega)} \\ &\le Ch(\|\mathcal{U}^V - \widetilde{\mathcal{U}}\|_{H^1(\Omega)} + \|\mathcal{U}^V - \mathcal{U}_h^V\|_{H^1(\Omega)}). \end{aligned} \tag{39}$$

Since $\|\mathcal{U}^V - \mathcal{U}_h^V\|_{H^1(\Omega)} = \mathcal{O}(h)$ has been proved, we require to bound $\|\mathcal{U}^V - \widetilde{\mathcal{U}}\|_{H^1(\Omega)}$.

$$\begin{aligned} \|\mathcal{U}^V - \widetilde{\mathcal{U}}\|^2_{H^1(\Omega)} &= A(\mathcal{U}^V - \widetilde{\mathcal{U}}, \mathcal{U}^V - \widetilde{\mathcal{U}}) \\ &= \lambda'(\Omega; \widetilde{\mathcal{U}} - \mathcal{U}^V)_\Omega - \lambda'(\Omega; \widetilde{\mathcal{U}} - \mathcal{U}^V)_{\Omega,h}. \end{aligned} \tag{40}$$

Using (30) with $\mathcal{X}_h$ replaced by $\mathcal{U}^V - \widetilde{\mathcal{U}}$, (40) implies that

$$\|\mathcal{U}^V - \widetilde{\mathcal{U}}\|_{H^1(\Omega)} \le Ch|u|^2_{W^{2,4}(\Omega)}.$$

Therefore, the conclusion holds. □

Lemma 5. *Let assumptions in Lemma 1 hold. Assume further that*

$$\|u\|_{W^{2,p}(\Omega)} \le Cp\lambda\|u\|_{L^p(\Omega)}$$

for $1 < p < \mu$ *with some* $\mu > d$ *and*

$$\|P_h u - u_h\|_{W^{1,\infty}(\Omega)} \le C|\log h|^{2/3}h|u|_{H^2(\Omega)}, \quad d = 3. \tag{41}$$

Then

$$\|u - u_h\|_{W^{1,\infty}(\Omega)} \le C|\log h|^{1-\frac{1}{d}}h|u|_{W^{2,\infty}(\Omega)}.$$

Proof. First, we split the error and use the triangle inequality to obtain

$$\|u-u_h\|_{W^{1,\infty}(\Omega)} \le \|u-P_hu\|_{W^{1,\infty}(\Omega)} + \|P_hu-u_h\|_{W^{1,\infty}(\Omega)}, \tag{42}$$

where $P_h : H_0^1(\Omega) \to V_h$ is defined in (15). In (42), the error estimate for the first term on the R.H.S. is standard (Corollary 8.1.12 [26]):

$$\|u-P_hu\|_{W^{1,\infty}(\Omega)} \le Ch|u|_{W^{2,\infty}(\Omega)}. \tag{43}$$

What left now is to estimate $\|P_hu-u_h\|_{W^{1,\infty}(\Omega)}$ for $d=2$. By the inverse inequality (see e.g., [26]), discrete Sobolev inequality (Lemma 4.9.2 of [26]) and Lemma 2, we obtain

$$\begin{aligned}\|P_hu-u_h\|_{W^{1,\infty}(\Omega)} &\le Ch^{-1}\|P_hu-u_h\|_{L^\infty(\Omega)}\\ &\le Ch^{-1}|\log h|^{1/2}\|\nabla(P_hu-u_h)\|_{L^2(\Omega)}\\ &\le C|\log h|^{1/2}h|u|_{H^2(\Omega)}. \quad \square\end{aligned} \tag{44}$$

Remark 1. To the best of our view, there is no similar result in 3D as the discrete Sobolev inequality in 2D. The proof thus cannot be performed for 3D In Lemma 5 and the assumption (41) is required. If we do not assume (41), then we obtain lower convergence rate for $d=3$. More precisely,

$$\begin{aligned}\|P_hu-u_h\|_{W^{1,\infty}(\Omega)} &\le Ch^{-3/2}\|\nabla(P_hu-u_h)\|_{L^2(\Omega)}\\ &\le C\sqrt{h}|u|_{H^2(\Omega)}\end{aligned}$$

by inverse inequality and Lemma 2.

Theorem 2. *Let assumptions in Theorem 1 hold. Assume further that $u \in W^{2,\infty}(\Omega)$. Then,*

$$\|\mathcal{U}^B-\mathcal{U}_h^B\|_{H^1(\Omega)} \le Ch|\log h|^{1-\frac{1}{d}}|u|_{W^{2,\infty}(\Omega)}.$$

Proof. The smoothness of domain Ω allows the problem (9) to be equivalent to the Neumann boundary value problem (21), i.e., $\mathcal{U}^B=\mathcal{U}^V$. Thus, we have $\mathcal{U}^B \in H^2(\Omega)^d$ by Lemma 4. We define the Ritz projection $P_h^B : \boldsymbol{V} \to \boldsymbol{V}_h$ and consider the variational problem: find $P_h^B\mathcal{U}^B \in \boldsymbol{V}_h$ such that

$$A(P_h^B\mathcal{U}^B, \mathcal{W}_h) = A(\mathcal{U}^B, \mathcal{W}_h) \quad \forall \mathcal{W}_h \in \boldsymbol{V}_h.$$

We have

$$\|\mathcal{U}^B-P_h^B\mathcal{U}^B\|_{H^1(\Omega)} \le Ch\|\mathcal{U}^B\|_{H^2(\Omega)}. \tag{45}$$

Then, we split $\mathcal{U}^B-\mathcal{U}_h^B = \mathcal{U}^B-P_h^B\mathcal{U}^B+P_h^B\mathcal{U}^B-\mathcal{U}_h^B$ and have

$$\|\mathcal{U}^B-\mathcal{U}_h^B\|_{H^1(\Omega)} \le \|\mathcal{U}^B-P_h^B\mathcal{U}^B\|_{H^1(\Omega)} + \|P_h^B\mathcal{U}^B-\mathcal{U}_h^B\|_{H^1(\Omega)}. \tag{46}$$

We now estimate $\|P_h^B\mathcal{U}^B-\mathcal{U}_h^B\|_{H^1(\Omega)}$. Denote $\mathcal{Y}_h := P_h^B\mathcal{U}^B-\mathcal{U}_h^B$. Then,

$$\begin{aligned}&\|\mathcal{Y}_h\|_{H^1(\Omega)}^2\\ &\le A(\mathcal{Y}_h,\mathcal{Y}_h)\\ &= A(\mathcal{U}^B-\mathcal{U}_h^B,\mathcal{Y}_h)\\ &= -\lambda'(\Omega;\mathcal{Y}_h)_{\partial\Omega}+\lambda'(\Omega;\mathcal{Y}_h)_{\partial\Omega,h},\\ &\le \|\mathcal{Y}_h\cdot n\|_{L^4(\partial\Omega)}\left(2\left\|\frac{\partial u}{\partial n}\frac{\partial(u-u_h)}{\partial n}\right\|_{L^{\frac{4}{3}}(\partial\Omega)}+\left\|\left|\frac{\partial u}{\partial n}-\frac{\partial u_h}{\partial n}\right|^2\right\|_{L^{\frac{4}{3}}(\partial\Omega)}\right)\\ &\le \|\mathcal{Y}_h\|_{L^4(\partial\Omega)}\left(2\left\|\frac{\partial u}{\partial n}-\frac{\partial u_h}{\partial n}\right\|_{L^{\frac{4}{3}}(\partial\Omega)}\left\|\frac{\partial u}{\partial n}\right\|_{L^\infty(\partial\Omega)}+\||\nabla u-\nabla u_h|^2\|_{L^{\frac{4}{3}}(\partial\Omega)}\right)\\ &\le |\partial\Omega|^{\frac{3}{4}}\|\mathcal{Y}_h\|_{L^4(\partial\Omega)}\big(2\|\nabla u-\nabla u_h\|_{L^\infty(\partial\Omega)}\|\nabla u\|_{L^\infty(\partial\Omega)}+\|\nabla u-\nabla u_h\|_{L^\infty(\partial\Omega)}^2\big).\end{aligned} \tag{47}$$

Considering that $u \in W^{2,\infty}(\Omega)$ and ∇u_h is piecewise constant on each element, we have further

$$\|\mathcal{Y}_h\|_{H^1(\Omega)}^2 \le |\partial\Omega|^{\frac{3}{4}}\|\mathcal{Y}_h\|_{L^4(\partial\Omega)}\big(2\|\nabla u-\nabla u_h\|_{L^\infty(\bar\Omega)}\|\nabla u\|_{L^\infty(\bar\Omega)}+\|\nabla u-\nabla u_h\|_{L^\infty(\bar\Omega)}^2\big), \tag{48}$$

in which

$$\begin{aligned}\|\mathcal{Y}_h\|_{L^4(\partial\Omega)} &\le C\|\mathcal{Y}_h\|_{W^{\frac{1}{2},2}(\partial\Omega)}\\ &\le C\|\mathcal{Y}_h\|_{H^1(\Omega)}\end{aligned} \tag{49}$$

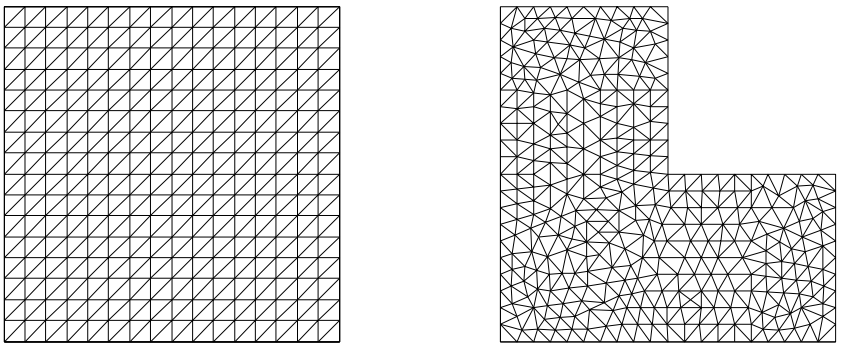

Fig. 1. One level of meshes used for the square and L-shaped domain.

by Sobolev embedding theorem. By (48) and (49), we obtain

$$\begin{aligned}\|\mathcal{Y}_h\|_{H^1(\Omega)} \leq & C|\partial\Omega|^{\frac{3}{d}}\left(2\|u-u_h\|_{W^{1,\infty}(\Omega)}\|u\|_{W^{1,\infty}(\Omega)}+\|u-u_h\|^2_{W^{1,\infty}(\Omega)}\right)\\ \leq & Ch|\log h|^{1-\frac{1}{d}}|u|_{W^{2,\infty}(\Omega)},\end{aligned} \tag{50}$$

where the continuity from Ω to $\bar{\Omega}$ and Lemma 5 are used. A combination of (45), (46) and (50) allows the conclusion to hold. □

4. Numerical results

We perform numerical experiments with FreeFem++ [30]. We consider only cases of the first (simple) Dirichlet eigenvalue and the first non-zero Neumann eigenvalue for simplicity. For more numerical examples involving high eigenvalue optimization as well as multiple cases, we refer to [24]. Examples corresponding to both Dirichlet and Neumann boundary conditions are presented. We choose two computational domains in $\mathbb{R}^2$: unit square and a L-shaped domain ($(-1,1)^2$ missing the upper right quarter). In Fig. 1, one level of triangulation is illustrated. To study h-convergence, uniform refinement is employed. The eigenfunction on square has enough smoothness, whereas the eigenfunction associated with the first eigenvalue on the L-shaped domain has a singularity at the reentrant corner. Lagrange Linear element is employed. We approximate the first Dirichlet eigenvalue and the first non-zero Neumann eigenvalue. We compute a numerical solution on a very fine mesh and use it as an "approximate" exact solution for reference in computing numerical errors. We also present shape optimization examples using a H^1 shape gradient algorithm. We calculate the volume integrals involved in the calculation of the volume Eulerian derivatives by numerical integration with Gaussian quadrature.

4.1. H^1 shape gradient flows

We present numerical shape gradients for both H^1-flows associated with the boundary and distributed Eulerian derivatives. In Fig. 2, the theoretical convergence rates are verified numerically on square. In Fig. 3, we see that the distributed shape gradient is nearly the same as the boundary shape gradient in the H^1 norm. But for the L^2 norm, higher and super-linear convergence rate and more accuracy can be observed. For the square with Neumann condition, we can see there is no advantage of distributed shape gradient in convergence and accuracy. The quadratic convergence of boundary shape gradient in L^2 norm is again unexpected. For the L-shaped domain with Neumann condition, similar phenomenon in Fig. 5 can be obtained as the Dirichlet case of Fig. 3. (See Fig. 4.)

4.2. Shape optimization

To demonstrate the performance of the shape gradients of H^1 flows, we solve numerically two shape optimization models in (2): minimizing the first Dirichlet eigenvalue and maximizing the first nonzero Neumann eigenvalue with prescribed fixed volume. Disk is the well-known optimal solution for each problem. We refer to [16] for numerical results when optimizing other Dirichlet eigenvalues with domain type Eulerian derivatives. We deal with the volume constraint by homothety [5,6] and consider the following unconstrained formulations instead:

$$\min_{\Omega \text{ is open}} \lambda|\Omega|^{\frac{2}{d}} \text{ (Dirichlet)} \quad \text{and} \quad \max_{\Omega \text{ is open}} \lambda|\Omega|^{\frac{2}{d}} \text{ (Neumann)}. \tag{51}$$

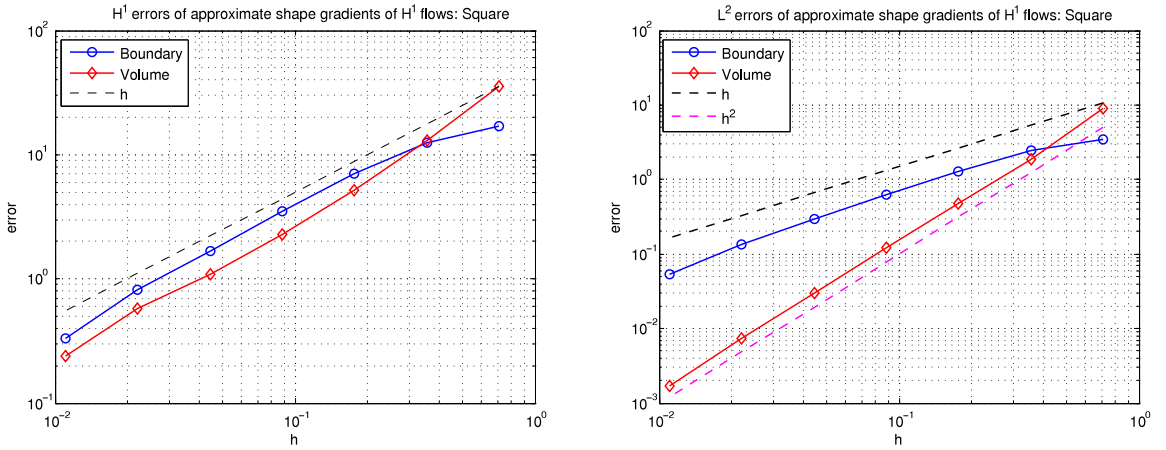

Fig. 2. Convergence history on errors of approximate shape gradients of H^1 flows: Square and Dirichlet boundary condition.

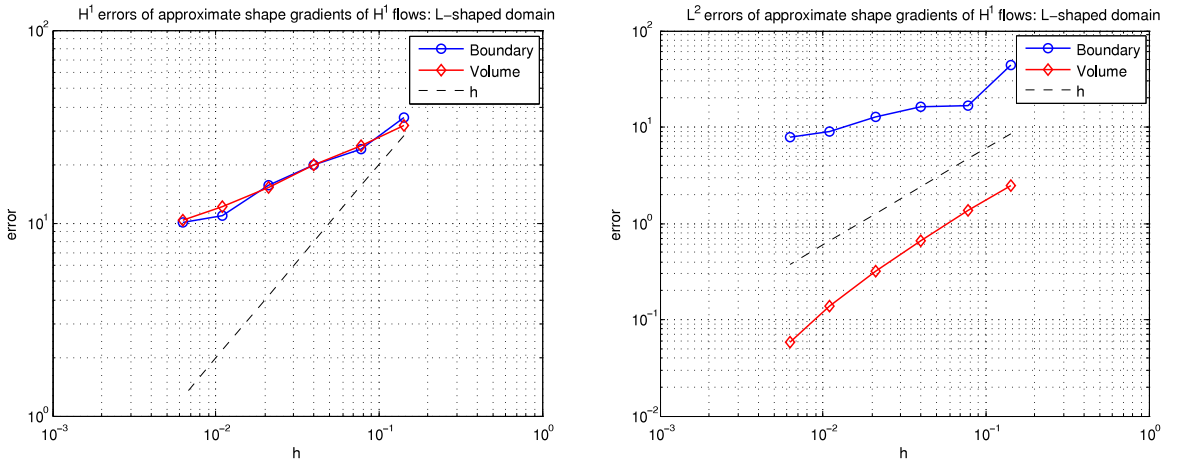

Fig. 3. Convergence history on errors of approximate shape gradients of H^1 flows: L-shaped domain and Dirichlet boundary condition.

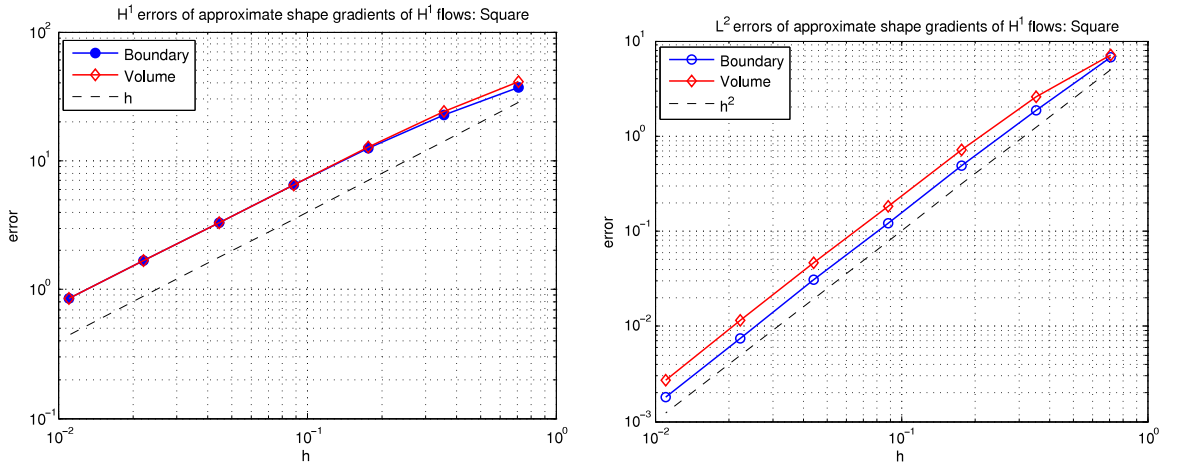

Fig. 4. Convergence history on errors of approximate shape gradients of H^1 flows: Square and Neumann boundary condition.

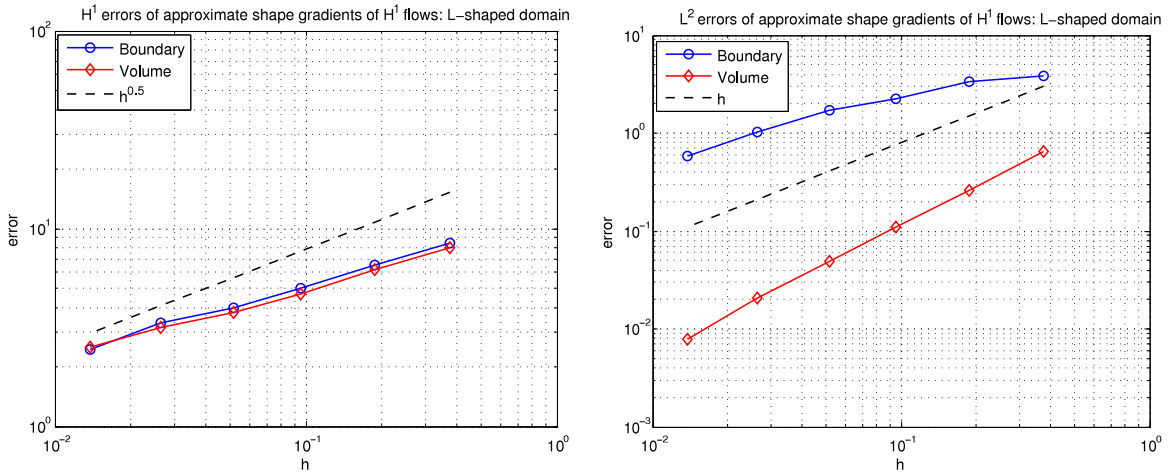

Fig. 5. Convergence history on errors of approximate shape gradients of H^1 flows: L-shaped domain and Neumann boundary condition.

The volume Eulerian derivatives of $\lambda|\Omega|$ for both cases are

$$\lambda'(\Omega;\mathcal{V})|\Omega|^{\frac{2}{d}}+\frac{2}{d}\lambda|\Omega|^{\frac{2}{d}-1}|\Omega|'=\int_{\Omega}\Big[\,|\Omega|^{\frac{2}{d}}\Big(-2\nabla u\cdot \mathrm{D}\mathcal{V}\nabla u+\mathrm{div}\mathcal{V}(|\nabla u|^2-\lambda u^2)\Big)+\frac{2}{d}\lambda|\Omega|^{\frac{2}{d}-1}\mathrm{div}\mathcal{V}\,\Big]\,\mathrm{d}x$$

by (5). The boundary Eulerian derivatives are

$$\int_{\partial\Omega}\left[-|\Omega|^{\frac{2}{d}}\left(\frac{\partial u}{\partial n}\right)^2+\frac{2}{d}\lambda|\Omega|^{\frac{2}{d}-1}\right]\mathcal{V}_n\mathrm{d}s \tag{52}$$

and

$$\int_{\partial\Omega}\left(|\Omega|^{\frac{2}{d}}(|\nabla_\Gamma u|^2-\lambda u^2)+\frac{2}{d}\lambda|\Omega|^{\frac{2}{d}-1}\right)\mathcal{V}_n\mathrm{d}s \tag{53}$$

for the Dirichlet and Neumann cases, respectively. We check numerically multiplicity of the eigenvalue using the rule with threshold in [2,6] and modify the Eulerian derivative if necessary. We observe that the multiplicity of the Neumann case is two during deformations. The linear combination of the first two (non-trivial) Neumann eigenvalues are considered as an objective, when they are close to each other. The gradient is modified correspondingly [6]. The step size should be chosen by trial and error for the objective to decrease. Set an initial step $\delta=1$ and a tolerance $\epsilon=10^{-4}$. At each iteration, we reduce the current step size by half repeatedly until it becomes feasible to avoid reversed triangles to appear during deformations. The algorithm we present below allows deformations only without topological changes. Shape gradient descent flow and ascending flow correspond to the Dirichlet case and Neumann case, respectively.

In order to evaluate better the performance of our algorithms for shape optimization, we compare the H^1 shape gradient flows with the traditional L^2 shape gradient flow (see e.g. [6]) in effectiveness and efficiency. The L^2 flow typically moves the boundary of the current domain according to the boundary Eulerian derivative. By (52)–(53), the L^2 flows require the "discrete" velocity fields to be

$$\mathcal{V}_h=-\left[-|\Omega|^{\frac{2}{d}}\left(\frac{\partial u_h}{\partial n}\right)^2+\frac{2}{d}\lambda_h|\Omega|^{\frac{2}{d}-1}\right]n$$

and

$$\mathcal{V}_h=\left[|\Omega|^{\frac{2}{d}}(|\nabla_\Gamma u_h|^2-\lambda_h u_h^2)+\frac{2}{d}\lambda_h|\Omega|^{\frac{2}{d}-1}\right]n$$

for gradient descent and ascent, respectively. The step size is determined similarly as in the H^1 flows. After the new boundary is determined, remeshing is required at each iteration. The computational cost for remeshing (even with a very fine mesh) is neglectable compared with that for the (nonlinear) eigenvalue forward solver.

In Fig. 6–7, we show that both shape gradients of H^1 descent flows and L^2 flow converge to the "right" optimal domain disk from the same initial square. If the initial domain is L-shape however, we can see from Fig. 8 that the volume H^1 flow converges to disk while the boundary H^1 flow fails due to the inaccurate shape gradient computation as proved and

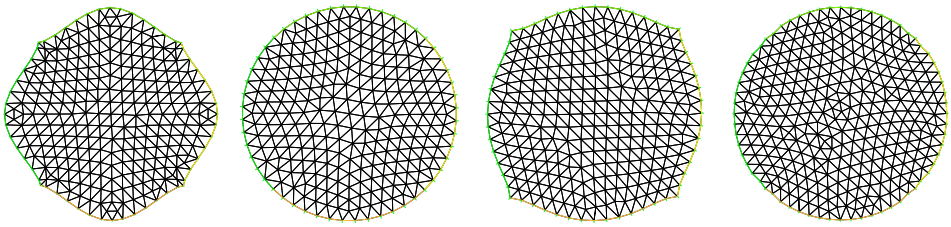

Fig. 6. Shape evolutions of the Dirichlet eigenvalue (from left to right): intermediate design, final result by volume Eulerian derivative, intermediate design, and final result by boundary Eulerian derivative (initial square in Fig. 1) (We refer to [24] for more other eigenvalue optimization examples).

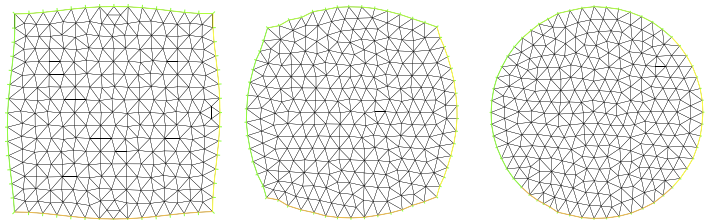

Fig. 7. Shape evolutions of the Dirichlet eigenvalue with the L^2 shape gradient flow from initial square: step 2, 5 and 15 (from left to right).

verified numerically above. Comparing with H^1 shape gradient flows, L^2 flow converges to disk as shown in Fig. 9 for shape evolutions. In Fig. 10 for the initial square case, the convergence history of objectives show that the volume H^1 shape gradient descent algorithm converges more efficiently than the boundary H^1 type. Both H^1 flows are more efficient than L^2 flow. For the initial L-shape case, the boundary H^1 flow fails. The volume H^1 flow converges more efficiently than the L^2 flow by counting and comparing the total costs of their corresponding algorithms. The algorithm with less iterations in optimization implies more efficiency when comparing the volume H^1 flows and L^2 flow. The volume H^1 flow requires less iterations than L^2 flow for shape optimization, although it requires to solve an additional elliptic problem besides an eigenvalue problem. We observe that the eigenvalue problem is nonlinear and the gradient flow problem is linear. The computational cost for solving former is less than that for solving latter.

For Neumann case, both algorithms associated with H^1 volume and boundary formulations converge to the right disk as shown in Fig. 11 with initial square. Fig. 12 shows that the L^2 flow is also effective. When starting with initial L-shape however, all H^1 and L^2 flows fail to converge to disk. For efficiency comparison, in Fig. 13 both H^1 flows are more efficient than the L^2 flow. No numerical evidence observed shows that the volume H^1 flow is more efficient or effective than the boundary H^1 flow. This is mainly because that the boundary H^1 shape gradient compared with the volume type is competitive in convergence rate as well as accuracy as noticed numerically above.

In Fig. 14 for 3D, the Dirichlet/Neumann eigenvalues are optimized effectively using the algorithms with volume H^1 shape gradients. We remark that the boundary H^1 flows fail to converge to the right ball for optimizing the Dirichlet eigenvalue, when the initial domain is L-shaped.

Algorithm 1: Boundary/Distributed shape gradient algorithm for eigenvalue optimization

Given an initial guess Ω_0, set $k = 0$, ϵ, δ;
while $|J(\Omega_{k+1}) - J(\Omega_k)| \geq \epsilon J(\Omega_k)$ **do**
  Solve the Dirichlet/Neumann eigenvalue problem;
  Solve the H^1 shape gradient flow;
  while *reversed triangle/tetrahedron appears* **do**
    $\delta \leftarrow \delta/2$;
  end
  Moving meshes: $\Omega_{k+1} \leftarrow \Omega_k + \delta \mathcal{U}_h$ with $\mathcal{U}_h = \mathcal{U}_h^V$ or $\mathcal{U}_h^B$;
  $k \leftarrow k + 1$;
end

5. Conclusions

We have performed convergence analysis for finite element approximations of boundary and distributed H^1 shape gradient flows for eigenvalue problems. For the Dirichlet case, theoretical analysis as well as numerical comparisons

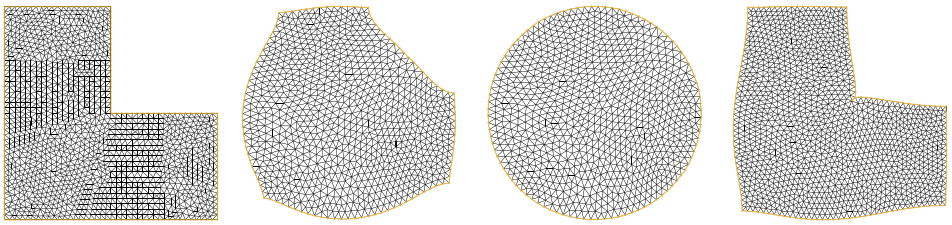

Fig. 8. Shape evolutions of the Dirichlet eigenvalue: initial domain (2672 triangles), intermediate domain, optimal domain with volume Eulerian derivative, and optimal domain with boundary Eulerian derivative (from left to right).

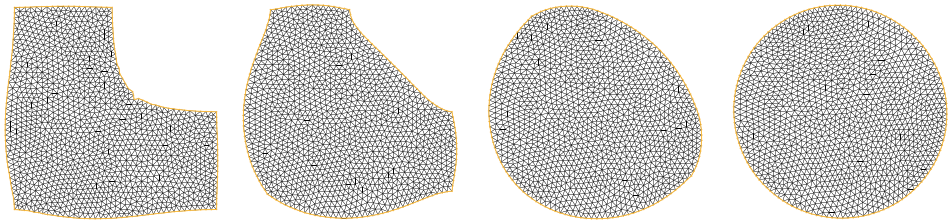

Fig. 9. Shape evolutions of the Dirichlet eigenvalue with the L^2 shape gradient flow: step 5, 20, 50, 150 (from left to right).

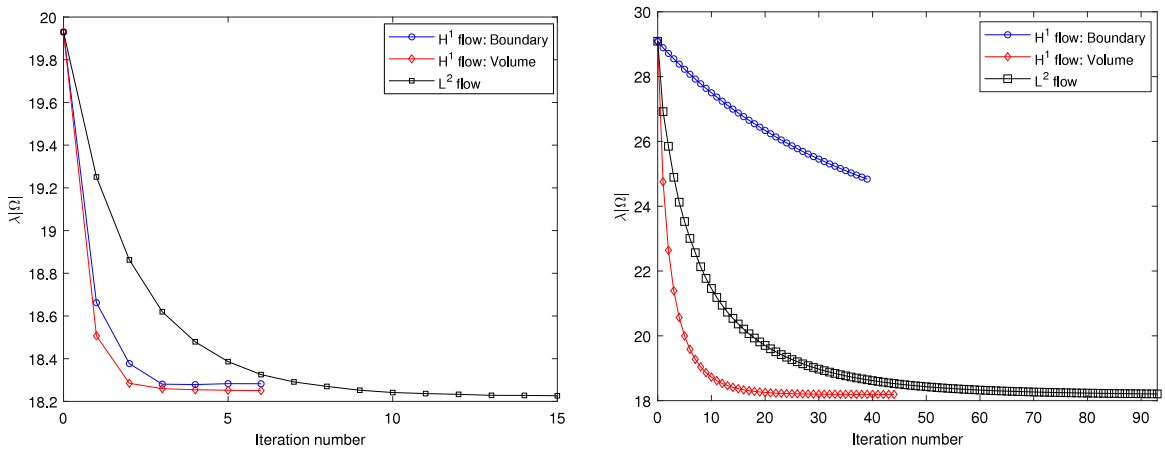

Fig. 10. Comparisons among L^2, boundary H^1, and volume H^1 shape gradient flows: convergence histories of shape functional for Dirichlet boundary condition with initial square (left) and initial L-shape (right).

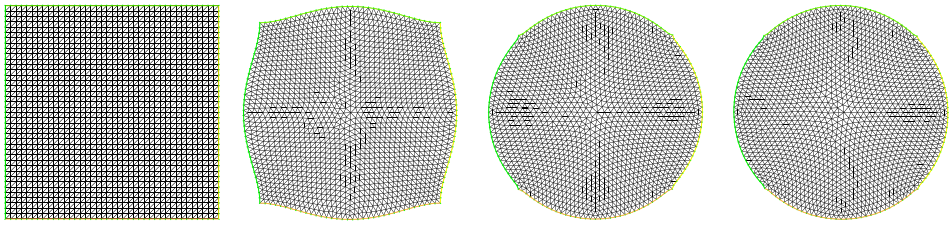

Fig. 11. Shape evolutions of the Neumann eigenvalue: initial domain (3200 triangles), intermediate domain, optimal domain with volume Eulerian derivative and optimal domain with boundary Eulerian derivative (from left to right).

have shown that the distributed shape gradient converges faster and offers higher accuracy. For the Neumann case, the boundary formulation is surprisingly competitive with the distributed type. Moreover, shape gradient algorithms are presented. Theoretical convergence analysis provides possible explanations for the effectiveness of the algorithms

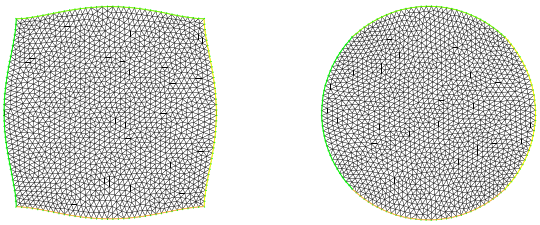

Fig. 12. Shape evolutions of the Neumann eigenvalue with L^2 shape gradient flows: intermediate domain and optimal domain.

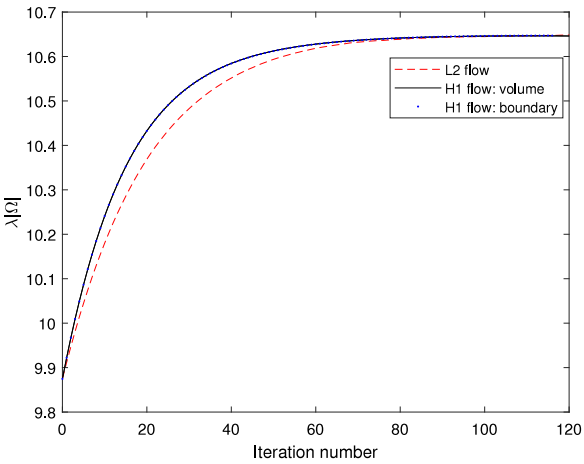

Fig. 13. Comparisons among L^2, boundary H^1, and volume H^1 shape gradient flows: convergence histories of shape functional for Neumann boundary condition with initial square.

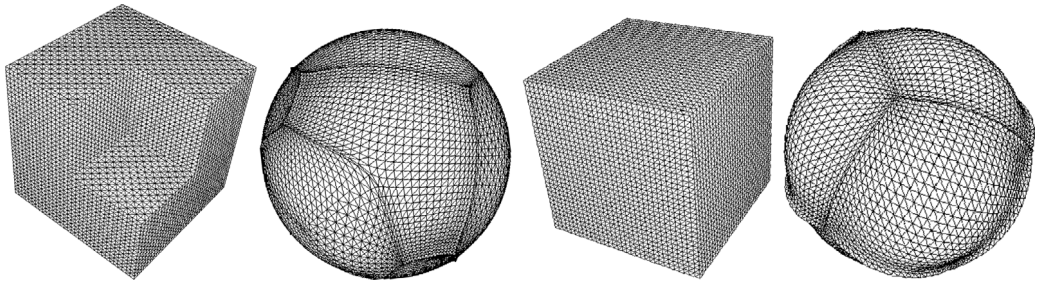

Fig. 14. Initial L-shaped domain (31841 mesh nodes) for optimizing Dirichlet eigenvalue, optimal domain, initial cube (35937 mesh nodes) for optimizing Neumann eigenvalue and its optimal domain (from left to right).

associated with different type shape gradients. For optimizing a Dirichlet eigenvalue, the distributed shape gradients are shown more effective. For maximizing a Neumann eigenvalue, the two type shape gradients perform equally well. Numerical evidence shows that the distributed H^1 shape gradient flow is more efficient than the boundary L^2 shape gradient flow in literature.

References

[1] G. Allaire, S. Aubry, F. Jouve, Eigenfrequency optimization in optimal design, Comput. Methods Appl. Mech. Engrg. 190 (2001) 565–3579.
[2] P.R.S. Antunes, P. Freitas, Numerical optimization of low eigenvalues of the Dirichlet and Neumann Laplacians, J. Optim. Theory Appl. 154 (2012) 235–257.
[3] D. Bucur, G. Buttazzo, Variational methods in shape optimization problems, in: Progr. Nonlinear Differential Equations Appl, Birkhäuser Boston, Inc., Boston, MA, 2005.
[4] M.C. Delfour, J.-P. Zolésio, Shapes and Geometries: Metrics, Analysis, Differential Calculus, and Optimization, second ed., SIAM, Philadelphia, 2011.
[5] A. Henrot, Extremum Problems for Eigenvalues of Elliptic Operators, Frontiers in Mathematics, Birkhauser, Basel, 2006.
[6] E. Oudet, Numerical minimization of eigenmodes of a membrane with respect to the domain, ESAIM Control Optim. Calc. Var. 10 (2004) 315–330.

[7] J. Sokołowski, J.-P. Zolésio, Introduction to Shape Optimization: Shape Sensitivity Analysis, Springer, Heidelberg, 1992.
[8] S. Zhu, Q. Wu, C. Liu, Variational piecewise constant level set methods for shape optimization of a two-density drum, J. Comput. Phys. 229 (2010) 5062–5089.
[9] E. Akhmetgaliyev, C.-Y. Kao, B. Osting, Computational methods for extremal Steklov problems, SIAM J. Cont. Optim. 55 (2017) 1226–1240.
[10] P.R.S. Antunes, E. Oudet, Numerical minimization of Dirichlet–Laplacian eigenvalues of fourdimensional geometries, SIAM J. Sci. Comput. 39 (2017) B508–B521.
[11] B. Bogosel, The method of fundamental solutions applied to boundary eigenvalue problems, J. Comput. Appl. Math. 306 (2016) 265–285.
[12] B. Osting, Optimization of spectral functions of Dirichlet–Laplacian eigenvalues, J. Comput. Phys. 229 (2010) 8578–8590.
[13] R.S. Jones, Computing ultra-precise eigenvalues of the Laplacian within polygons, Adv. Comput. Math. 43 (2017) 1325–1354.
[14] T. Betcke, L.N. Trefethen, Reviving the method of particular solutions, SIAM Rev. 47 (2005) 469–491.
[15] S. Wu, X. Hu, S. Zhu, A multi-mesh finite element method for phase-field based photonic band structure optimizatiom, J. Comput. Phys. 357 (2018) 324–337.
[16] S. Zhu, X. Hu, Q. Wu, A level set method for shape optimization in semilinear elliptic problems, J. Comput. Phys. 355 (2018) 104–120.
[17] M. Berggren, A unified discrete-continuous sensitivity analysis method for shape optimization, in: Applied and Numerical Partial Differential Equations, Springer, 2010, pp. 25–39.
[18] B. Osting, C.Y. Kao, Minimal convex combinations of sequential Laplace–Dirichlet eigenvalues, SIAM J. Sci. Comput. 35 (2013) B731–B750.
[19] R. Hiptmair, A. Paganini, S. Sargheini, Comparison of approximate shape gradients, BIT 55 (2015) 459–485.
[20] S. Zhu, Z. Gao, Convergence analysis of mixed finite element approximations to shape gradients in the Stokes equation, Comput. Methods Appl. Mech. Engrg. 343 (2019) 127–150.
[21] E. Burman, D. Elfverson, P. Hansbo, M. Larson, K. Larsson, Shape optimization using the cut finite element method, Comput. Methods Appl. Mech. Engrg. 328 (2018) 242–261.
[22] A. Laurain, K. Sturm, Distributed shape derivative via averaged adjoint method and applications, ESAIM Math. Model. Numer. Anal. 50 (2016) 1241–1267.
[23] V. Schulz, M. Siebenborn, K. Welker, Structured inverse modeling in parabolic diffusion problems, SIAM J. Control Optim. 53 (2015) 3319–3338.
[24] S. Zhu, Effective shape optimization of Laplace eigenvalue problems using domain expressions of Eulerian derivatives, J. Optim. Theory Appl. 176 (2018) 17–34.
[25] S. Zhu, X. Hu, Convergence analysis of Galerkin finite element approximations to shape gradients in eigenvalue optimization, arXiv preprint arXiv:1807.00265.
[26] S.C. Brenner, L.R. Scott, The Mathematical Theory of Finite Element Methods, third ed., Springer, New York, 2008.
[27] H. Xie, A multigrid method for eigenvalue problem, J. Comput. Phys. 274 (2014) 550–561.
[28] A. Knyazev, J. Osborn, New a priori FEM error estimates for eigenvalues, SIAM J. Numer. Anal. 43 (2006) 2647–2667.
[29] I. Babuska, J. Osborn, Finite element-Galerkin approximation of the eigenvalues and eigenvectors of selfadjoint problems, Math. Comp. 52 (1989) 275–297.
[30] F. Hecht, O. Pironneau, A.L. Hyaric, K. Ohtsuka, Freefem++ Manual, 2006.